METHODS FOR THE RETRIEVAL OF MICROPHYSICAL AEROSOL PARAMETERS FROM OPTICAL DATA

Christine Böckmann[1], **Andreas Kirsche**[1], **Christoph Ritter**[2]

[1]*Institute of Mathematics, Potsdam University, Am Neuen Palais 10, 14469 Potsdam, Germany, E-mail:bockmann@rz.uni-potsdam.de, kirsche@rz.uni-potsdam.de*

[2]*Alfred Wegener Institute for Polar- and Marine Research, Telegrafenberg A43, 14473 Potsdam, Germany, E-mail:critter@awi-potsdam.de*

ABSTRACT

We propose two new possibilities to improve the retrieval accuracy of microphysical particle parameters, in particular, the total number concentration. For monomodal-lognormal number distributions we suggest a least squares method (LSM) procedure whereas for arbitrary shaped distributions a maximum entropy method (MEM) seems to be favourable. Numerical simulation examples show the improvements. Finally, the modified methods were tested for measurement cases.

1. INTRODUCTION

Aerosols are one of the key uncertainties influencing the Earth's radiation budget and require therefore a detailed characterization of optical and physical properties to improve the modelling of the planet's radiation forcing. In this regard, there is a need to determine microphysical aerosol particle properties by inversion using optical data. The inversion problem in a mathematical sense is ill-posed. Its solution requires the application of appropriate mathematical regularization techniques. The performances of some regularization algorithms for lidar remote sensing were discussed by [1], [2], [3] and [4]. The mathematical ill-posed model which relates the optical and the physical particle parameters, consists of a Fredholm system of two integral equations of the first kind for the backscatter and extinction coefficients

$$\Gamma(\lambda) = \int_{r_0}^{r_1} K^{\mathrm{n}}_{\pi/\mathrm{ext}}(\lambda, r; m, s)\; n(r)\; dr \qquad (1)$$

where r denotes the particle radius, m is the complex refractive index, assumed wavelength- and size-independent, s is the shape of the particles, r_0 and r_1 represent suitable lower and upper limits, respectively, of realistic particle radii, λ is the measurement wavelength, n is the particle number distribution, $K^{\mathrm{n}}_{\mathrm{ext}}(\lambda, r; m) = \pi r^2 Q_{\mathrm{ext}}(\lambda, r; m)$ is the backscatter and $K^{\mathrm{n}}_{\pi}(\lambda, r; m) = \pi r^2 Q_{\pi}(\lambda, r; m)$ is the extinction number kernel. $Q_{\pi/\mathrm{ext}}(\lambda, r; m)$ are the backscatter and the extinction efficiency, respectively, for more details see e.g. [3]. The kernel functions reflect shape, size, and material composition of the particles. Here homogeneous spherical particles, i.e., Mie scattering theory, are considered, which gives a reasonable approximation for some kind of aerosol. Γ in Eq. (1) stands for the backscatter coefficient β and/or the extinction coefficient α, respectively, depending on the measurement data. However, one is mostly interested in the following microphysical parameters like the volume and surface-area concentration, the effective radius and the total number concentration

$$a_{\mathrm{t}} = 3 \int \frac{v(r)}{r}\, \mathrm{d}r, \quad v_{\mathrm{t}} = \int v(r)\, \mathrm{d}r,$$

$$r_{\mathrm{eff}} = 3\frac{v_{\mathrm{t}}}{a_{\mathrm{t}}} \quad \text{and} \quad n_{\mathrm{t}} = \frac{3}{4\pi} \int \frac{v(r)}{r^3}\, \mathrm{d}r \qquad (2)$$

with

$$v(r) = \frac{4\pi r^3}{3}\, n(r)\,. \qquad (3)$$

The parameter n_{t} is, e.g., a very important input value for local climate models like HIRAM [5]. But, unfortunately, it is the most sensitive parameter in the retrieval. This was remarked or, therefore, it was omitted in [1] and [2] or [3] and [4], respectively. In Ref. [2], e.g., for the worse case 70% error is noted. Furthermore, [1] and [3] found that the regularized inversion is more stable by using the volume integral equation, i.e. substituting Eq. (3) into Eq. (1). Since the retrieval $\tilde{v}(r)$ for the volume distribution $v(r)$ is only an estimation with some noise level a great amplification of this noise level occurs in determining n_{t} by Eq. (2), i.e., in dividing by r^3 for $r \to 0$. In the following we write $v(r)$ instead of $\tilde{v}(r)$ for simplicity. The paper focuses on the improvement of the retrieval of n_{t}. Two different methods will be considered.

2. METHODOLOGIES

We propose two algorithms for improving the determination of the total number concentration n_{t}. The first step in both algorithms consists in using the regularized inversion to determine an estimation of the volume distribution $v(r)$, see [3] and [4] for two different regularization possibilities. The second step consists in the improved determination of the microphysical particle parameters without using directly the Eq. (2).

2.1. Least Squares Method

In case that one discovers in the first retrieval step that the estimated distributions $n(r)$ and $v(r)$, respectively, look similar to a monomodal-lognormal distribution, i.e.

$$n_{\rm M}(r; n_{\rm t}, r_{\rm med}, \sigma) = \frac{n_{\rm t}}{\sqrt{2\pi}\ln\sigma}\ \frac{1}{r}\ \exp\left\{-\frac{\ln^2\frac{r}{r_{\rm med}}}{2\ln^2\sigma}\right\}$$

and

$$v_{\rm M}(r; n_{\rm t}, r_{\rm med}, \sigma) = \frac{2\sqrt{2\pi}}{3}\frac{n_{\rm t}}{\ln\sigma}\ r^2 \exp\left\{-\frac{\ln^2\frac{r}{r_{\rm med}}}{2\ln^2\sigma}\right\},$$

it is possible to continue in the second step with a nonlinear least squares fitting to a monomodal-lognormal distribution. We know the estimation of $v(r)$ at m different tuples $(r_j; v_j),\ i = 1, .., m$. We are interested in estimating the three parameters $x = (n_{\rm t}, r_{\rm med}, \sigma)$. Therefore, on has to minimize the functional

$$\Phi(x) = \|v(.) - v_M(., x)\|_2 = \sqrt{\sum_{j=1}^{m} |v_j - v_M(r_j, x)|^2}$$

by using, e.g., the modified Gauss-Newton method for separable least squares problems, see [6]. Firstly, one splits off the linear parameter $n_{\rm t}$, i.e., $v_{\rm M}(r, x) = n_{\rm t} \cdot \hat{v}_{\rm M}(r, y), y = (r_{\rm med}, \sigma)$. It holds

$$n_{\rm t}(y) = \frac{\sum\limits_{j=1}^{m} \hat{v}_{\rm M}(r_j, y)\ v_j}{\sum\limits_{j=1}^{m} \hat{v}^2_{\rm M}(r_j, y)}$$

and, therefore, it is enough to minimize $\hat{\Phi}(y) = \|v - n_{\rm t}(y) \cdot \hat{v}_{\rm M}(., y)\|_2$ by using a suitable initial value $y_0 = (r_{\rm med_0}, \sigma_0)$. It is favourable to determine the initial value by using the data points $(r_j; v_j),\ i = 1, .., m$. It holds

$$\ln\sigma = \frac{1}{\sqrt{2}}\sqrt{-\frac{(\ln r - \ln r_{\rm max})^2}{\ln v_{\rm M}(r) - \ln v_{\rm M}(r_{\rm max})}}\ \text{ for }\ \sigma > 1.$$

where $v_{\rm M}(r_{\rm max})$ is the maximum value of the function $v_{\rm M}$. In using the maximum value of v_j, i.e. $v_{j_{\rm max}},\ j_{\rm max} \in \{1, ..., m\}$, we receive for each data tuple $(r_i, v_i),\ i = 1, ..., m,\ i \neq j_{\rm max}$ an estimation for $\ln\sigma_i$. Moreover, the mean value $\ln\sigma_0 = (\sum_{i=1}^{m} \ln\sigma_i)/(m-1)$ with $i \neq j_{\rm max}$ gives a suitable initial value σ_0. Furthermore, one gets a good initial value for $r_{\rm med}$ with $r_{\rm med_0} = r_{j_{\rm max}} \cdot \exp(-2\ln^2\sigma_0)$. Finally, the fitting parameters are $r^{\rm Fit}_{\rm med}$, $\sigma^{\rm Fit}$ and $n^{\rm Fit}_{\rm t} = n_{\rm t}(r^{\rm Fit}_{\rm med}, \sigma^{\rm Fit})$ and one gets the improved microphysical particle parameters by

$$\begin{aligned} r_{\rm eff} &= r^{\rm Fit}_{\rm med} \cdot \exp\left\{\frac{5}{2}\ln^2\sigma^{\rm Fit}\right\}, \quad n_{\rm t} = n^{\rm Fit}_{\rm t} \quad (4)\\ a_{\rm t} &= 4\pi\ n^{\rm Fit}_{\rm t}\ (r^{\rm Fit}_{\rm med})^2 \cdot \exp\left\{2\ln^2\sigma^{\rm Fit}\right\} \quad \text{and}\\ v_{\rm t} &= \frac{4\pi}{3}\ n^{\rm Fit}_{\rm t}\ (r^{\rm Fit}_{\rm med})^3 \cdot \exp\left\{\frac{9}{2}\ln^2\sigma^{\rm Fit}\right\}, \end{aligned}$$

see [7]. Since the retrievals for $r_{\rm eff}, a_{\rm t}$ and $v_{\rm t}$ show already good accuracies in the first step, see [3], we only expect an improvement for $n_{\rm t}$.

2.2. Maximum Entropy Method

In case that we do not discover a monomodal log-normal distribution in the first step, i.e. we find an arbitrary distribution possibly with more than one mode, we suggest an improvement by using a particular MEM. Firstly, we regard the integral equation (1) with the number distribution $n(r) = n_0(r)$ as usual and, additionally, with the so called moment distribution $n_g(r) = r^g \cdot n(r),\ g > 0$,

$$\Gamma(\lambda) = \int_{r_0}^{r_1} \frac{\pi}{r^{g-2}}\ Q_{\pi/\rm ext}(\lambda, r; m)\ n_g(r)\ {\rm d}r, \qquad (5)$$

$g = 0, 1, 2, ..,$, similar to [2]. Discretization of the integral equation (5) via collocation, see [3], yields for each $g \in N$ in a linear equation system

$$T^g_{\pi/\rm ext} N_g = \Gamma + \epsilon \qquad (6)$$

with vectors $N_g = (n_{g,1}, ..., n_{g,p})$ and $\Gamma = (\Gamma_1, ..., \Gamma_p)$ as well as a matrix $T^g_{\pi/\rm ext}$ with elements $T^g_{j,i} := \{T^g_{\pi/\rm ext}\}_{j,i}$. The estimation for the moment distribution is a linear combination $n_g(r) = \sum_{i=1}^{p} n_{g,i}\ \varphi_i(r)$ where φ_i are p B-spline functions of order 4 (piecewise cubic polynomials) with equidistant nodes. In using this moment distributions we can estimate the moments $M_k = \int n_k(r){\rm d}r$ of $n(r)$ and it holds $n_{\rm t} = M_0,\ a_{\rm t} = 4\pi\ M_2,\ v_{\rm t} = \frac{4\pi}{3}\ M_3$ and $r_{\rm eff} = \frac{M_3}{M_2}$. We assume that the kth moment of $n(r) = \sum_{i=1}^{p} n_{0,i}\varphi_i(r)$ is known and we get

$$M_k = \int r^k\ n(r){\rm d}r = \sum_{i=1}^{p} n_{0,i} \int r^k \varphi_i(r){\rm d}r = \sum_{i=1}^{p} n_{0,i} s^k_i$$

with $s^k_i = \int r^k \varphi_i(r){\rm d}r$. Let φ^ν_i normalized with respect to $s^\nu_i,\ \nu \in N$, i.e. $\varphi^\nu_i = \varphi_i / s^\nu_i$ and we are looking for $n(r)$ with respect to this basis, i.e. $n(r) = \sum_{i=1}^{p} n^\nu_{0,i}\varphi^\nu_i(r)$. Then $k = \nu$ yields $M_k = \sum_{i=1}^{p} n^k_{0,i}$.

Secondly, we introduce the entropy functional. With its ultimate roots in 19th century statistical mechanics and a subsequent strong justification based upon probability theory, the MEM has provided an extremely successful variational principle to address this type of inversion problems. The starting point of our approach is to use a discretized form of the Shannon entropy functional Ω, see e.g. [8],

$$\Omega(N^k_0) = \sum_{i=1}^{p} n^k_{0,i} \ln(n^k_{0,i}) \qquad (7)$$

which one has to minimize under the two constraints that, firstly, Eq. (6) holds for $g = 0$ with respect to the basis $\{\varphi^k_i\}$ and, secondly, $M_k = \sum_{i=1}^{p} n^k_{0,i}$. This is an ordinary mathematical optimization problem with equality constraints only, since $n^k_{0,i} > 0$ holds automatically because of the functional definition in (7). Those constrained problems can be reduced to an unconstrained convex optimization problem via the Lagrangian multiplier method, see e.g. [9]. We use the common Lagrangian functional with Lagrangian multiplies λ_j,

$$L(n, \lambda) = \Omega(N^k_0) + \bar{\lambda}_0 \left(\sum_{i=1}^{p} n^k_{0,i} - M_k\right) +$$

$$+ \quad \sum_{t=1}^{m} \lambda_t \left(\sum_{i=1}^{n} T_{t,i}^0 n_{0,i}^k - \Gamma_t \right)$$

which one has to minimize. For the partial derivatives hold

$$\frac{\partial}{\partial n_{0,i}^k} L(n, \lambda) = \ln(n_{0,i}^k) + \lambda_0 + \sum_{t=1}^{m} \lambda_t T_{t,i}^0$$

with $\lambda_0 = 1 + \bar{\lambda}_0$. The necessary condition yields

$$n_{0,i}^k = \exp\left\{ -\sum_{j=1}^{m} \lambda_j T_{j,i}^0 \right\} / \exp(\lambda_0).$$

and with $M_k = \sum_{i=1}^{p} n_{0,i}^k$ one obtains

$$\exp(\lambda_0) = \frac{1}{M_k} \sum_{z=1}^{p} \exp\left\{ -\sum_{t=1}^{m} \lambda_t T_{t,z}^0 \right\}$$

and, moreover,

$$n_{0,i}^k = \frac{M_k \exp\left\{ -\sum_{t=1}^{m} \lambda_t T_{t,i}^0 \right\}}{\sum_{z=1}^{p} \exp\left\{ -\sum_{t=1}^{m} \lambda_t T_{t,z}^0 \right\}}. \qquad (8)$$

Substituting Eq. (8) into the Eq. (6) one gets

$$\begin{aligned} 0 &= \sum_{i=1}^{p} T_{j,i}^0 n_{0,i}^k - \Gamma_j = \sum_{i=1}^{p} \left(T_{j,i}^0 - \Gamma_j / M_k \right) n_{0,i}^k \\ &= \sum_{i=1}^{p} \left(M_k T_{j,i}^0 - \Gamma_j \right) \exp\left\{ -\sum_{t=1}^{m} \lambda_t T_{t,i}^0 \right\} \qquad (9) \end{aligned}$$

for $j = 1, ..., m$. This nonlinear equation system can be solved again with the algorithm proposed in [6] to get the multipliers λ_t. This method is able to find a solution by using an arbitrary known moment M_k.

Finally, we adapt the proposed method to determine microphysical parameters by using the third moment $M_3 = 3/(4\pi) v_{\mathrm{t}}$ of the distribution $n(r)$ since the estimation of v_{t} is the most stable one, see [3]. Therefore, by using M_3, i.e. $k = 3$, and the normalized B-spline functions φ_i^1, i.e. $\nu = 1$, we are looking for an estimation of $n_2(r)$ contained in the space $\mathrm{span}\{\varphi_1^1, ..., \varphi_p^1\}$, i.e. $n_2(r) = \sum_{i=1}^{p} n_{2,i}^1 \varphi_i^1(r)$ with

$$M_3 = \int_0^\infty r \cdot n_2(r)\, \mathrm{d}r = \sum_{i=1}^{p} n_{2,i}^1 \int_0^\infty r \cdot \varphi_i^1(r)\, \mathrm{d}r = \sum_{i=1}^{p} n_{2,i}^1.$$

Next, we modify the Eq. (8) to

$$n_{2,i}^1 = \frac{M_3 \exp\left\{ -\sum_{t=1}^{m} \lambda_t T_{t,i}^2 \right\}}{\sum_{z=1}^{p} \exp\left\{ -\sum_{t=1}^{m} \lambda_t T_{t,z}^2 \right\}}$$

and in the same way the nonlinear Eq. (9) to compute the particular λ_t. Then we can determine $M_2 = \int n_2(r)\, \mathrm{d}r$. Repeating this procedure for M_1 and $M_0 = n_{\mathrm{t}}$ we get a better estimation for n_{t} than by using directly Eq. (2).

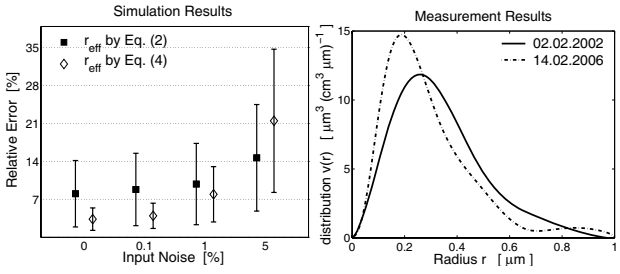

Figure 1. Comparison of the retrieval results for the effective radius. The uncertainty bars correspond to the standard deviation (left). The retrieved volume distributions for the measurement cases by using regularized inversion. The additional fit is not shown (right).

Table 1. Comparison of the retrieval results for the total number concentration n_{t}

Input Noise	Mean relative error of n_{t} (%)	
(%)	by a fit see Eq. (4)	by using Eq. (2)
0.00	16 ± 009	20600 ± 38500
0.10	19 ± 010	20000 ± 37700
1.00	52 ± 108	18700 ± 36900
5.00	58 ± 031	15300 ± 27500

3. NUMERICAL TESTS AND APPLICATIONS

3.1. Simulation Results

Firstly, a simulation test for LSM was done with monomodal-lognormal number distributions, known refractive index, 6 backscatter coefficients (at 355 nm, 400 nm, 532 nm, 710 nm, 800 nm und 1064 nm) and 2 extinction coefficients (at 355 nm and 532 nm) with the following values $\sigma = 1.4,\ 1.8,\ 1.3$ and $r_{\mathrm{med}} = 0.1,\ 0.1,\ 0.3\ \mu\mathrm{m}$ as well as $n_{\mathrm{t}} = 1,\ 1,\ 1\ \mathrm{cm}^{-3}$. For the refractive index m we used for the real part $\mathrm{Re}(m) = 1.4,\ 1.5,\ 1.7$ and for the imaginary part $\mathrm{Im}(m) = 0,\ 0.005,\ 0.01$. In sum 27 simulation examples were investigated. In simulating the noise levels Gaussian noise was used, i.e. each coefficient was disturbed with e.g. 5% normal distributed noise. To increase the statistical significance for each noise level 100 representants were produced. As regularization technique the hybrid Padé method of [10] with discrepancy principle as parameter choice rule was used. From those retrieved volume distributions the parameters r_{eff} and n_{t} were computed by Eq. (2). Subsequently, LSM was used to determine r_{eff} and n_{t}. The results are shown in Fig. 1 (left) and Table 1. As expected the fitting procedure does not improve the error of the effective radius so much. Both retrievals are more or less in the same order of magnitude, see Fig. 1. But there is a huge improvement for the total number concentration, see Table 1.

Secondly, one first simulation test for a sun photometer case with noiseless input data was made for MEM in using a monomodal-lognormal number distribution with the following parameter values $\sigma = 1.6, r_{\mathrm{med}} = 0.1\ \mu\mathrm{m}$ and $n_{\mathrm{t}} = 123\ \mathrm{cm}^{-3}$, a known refractive index $m = 1.5 + 0.01\mathrm{i}$ as well as 100 extinction coefficients (wavelengths

equidistant distributed between 355 nm and 1064 nm). That is justified here since a sun photometer has several channels, e.g. 17 at AWI station, which are sufficient to make a good cubic spline interpolation to get 100 data points. Thereby, the third moment v_{t} was determined with an accuracy of 4% in using the Padé method [10] for the first step. Again, whereas the parameters r_{eff} and a_{t} maintained their accuracies in the second step by using MEM a huge improvement for the total number concentration occurs, i.e. the retrieved value is $n_{\mathrm{t}} = 156\ \mathrm{cm}^{-3}$ with an error of only 27.2% having in mind that LSM used additionally a-priori information about the distribution shape. Further extensive investigations have to be made for MEM. This is still an ongoing work.

3.2. Measurement Results

The first data set presented here was recorded on 02.03.2002 with a Raman lidar (3 backscatter wavelengths at 355 nm, 532 nm and 1064 nm as well as 2 extinction wavelengths at 355 nm and 532 nm), operating at the Koldewey station, Spitsbergen at $78.9°$ North and $11.9°$ East during an arctic haze event. Lidar profiles were averaged over 60 m and 2 hours time (during 1UT to 3UT) in very stable meteorological conditions. The retrieval of backscatter and extinction coefficients was done according to the classic Raman lidar evaluation proposed by [11]. At an altitude of 1555 m increased values of extinction and backscatter were found, accompanied by considerable low values of the volume depolarization, which indicates almost spherical particles.
From these lidar data a mean refractive index of $(1.69 \pm 0.04) + (0.026 \pm 0.005)$i could be estimated. For, e.g., 1.65+0.035i the solution appears after regularized inversion as a monomodal and lognormal-like distribution, see Fig. 1 (right), hence, we used a monomodal lognormal distribution for LSM. With this method we estimated $n_{\mathrm{t}}^{\mathrm{Fit}} = 89$ per cm^3 and an effective radius of $0.23\ \mu\mathrm{m}$.
This effective radius and a monomodal particle number distribution matches to aged aerosol as well. So our data evaluation scheme is able to reproduce the characteristics of arctic haze. The air probed on this day came from Northern Romania, Ukraine and Russia in the 8 days before its arrival in Spitsbergen as was confirmed with NOAA hysplit trajectories [12]. Hence, anthropogenic pollutants can be expected and the index of refraction is in agreement with a mixture of sulphates and soot, which have been found as main constituencies of arctic haze by particle counters during prior campaigns at the site.
The data for the second example comes from 14.02.2006 at 1775 m. It was recorded at the same site with the same lidar as before between 11:30 and 12:45 UT. Data again was averaged over 60 m and the whole time period. In this case an anthropogenic influence of the air masses is not so obvious from NOAA hysplit. However, the air which arrived in Spitsbergen at 1775 m passed over the coastline of Alaska and then Siberia at low heights some days before, where it may have taken up some aerosol. In accordance with a less pronounced anthropogenic impact in this data set we found a lower index of mean refraction of $(1.61 \pm 0.041) + (0.006 \pm 0.0046)$i, which is nevertheless still higher than pure sulphate particles alone. Again volume depolarization was low, so that Mie theory of scattering could be applied. For, e.g., 1.59+0.015i as expected for arctic aerosol a monomodal volume distribution was obtained for this case as well. Therefore again the LSM was used for the retrieval of the microphysical properties. Here more but smaller particles were found: $n_{\mathrm{t}}^{\mathrm{Fit}} = 285$ per cm^3 and $r_{\mathrm{eff}} = 0.20\ \mu\mathrm{m}$. The smaller diameter of the aerosol in this second example can probably be explained by its longer residence time in the atmosphere (around 10 days, compared to 6 days in our first case).
For both data sets even an estimation of the single scattering albedo, which is a very important quantity in climatological models, can be given. A value of 0.834 and 0.927, respectively, was found for 532 nm. So the retrieval of the microphysical parameters of arctic aerosol by inversion of lidar data is possible. This tool will greatly help to monitor and understand climatological processes even at remote and sensitive sites as the arctic ecosystem.
Acknowledgments: This work was supported by the PEP Project from the HGF "Impuls und Vernetzungsfond" under the grant VH-VI-100 and by the European Commission with respect to the EARLINET-ASOS Project under grant 025991 (RICA).

REFERENCES

1. Müller, D., Wandinger, U., Ansmann, A., Microphysical particle parameters from extinction and backscatter data by inversion with regularization: simulation. *Appl. Opt.*, 38:2358–2368, 1999.
2. Veselovskii, I., Kolgotin, A., Griaznov, V., Müller, D., Franke, K., et al., Inversion of multiwavelength Raman lidar data for retrieval of bimodal aerosol size distribution. *Appl. Opt.*, 43:1180–1195, 2004.
3. Böckmann, C., Mironova, I., et al., Microphysical aerosol parameters from multiwavelength lidar. *J. Opt. Soc. Am. A*, 22:518–528, 2005.
4. Böckmann, C. and Kirsche, A., Iterative regularization method for lidar remote sensing. *Comput. Phys. Comm.*, 174:607–615, 2006.
5. Dethloff, K., Rinke, A., Lehmann, R., Christensen, J.H., et al., Regional climate model of the arctic troposphere. *JGR*, 101:23401–23422, 1996.
6. Böckmann, C., Curve fitting of physical spectra. *J. Comput. Appl. Math.*, 70:207–224,1996.
7. Seinfeld, J.H. and Pandis, S.N., *Atmospheric Chemistry and Physics*. John Wiley, New York, 1998.
8. Troyan, V. and Hayakawa, M., *Inverse Geophysical Problems*. TERRAPUB, 2002.
9. Quarteroni, A., Sacco, R., and Sateri, F., *Numerical Mathematics*. Springer Verlag, New York, 2000.
10. Kirsche, A., Böckmann, C., Padé iteration method for regularization. *Appl. Math. Comp.*, in press 2006.
11. Ansmann, A., Wandinger, et al., Independent measurements of extinction and backscatter profiles in cirrus clouds by using a combined Raman elastic-backscatter lidar. *Appl. Opt.*, 31:7113–7131, 1992.
12. Draxler, R.R., Rolph, G.D., HYSPLIT model. *NOAA Air Ressources Laboratory, Silver Spring, MD*, http://www.arl.noa.gov/ready/hysplit4.html, 2003.